Electronic Supplementary Material (ESI) for New Journal of Chemistry.

Tuning heterostructure in nanofibers by annealing temperature for high performance lithium-ion batteries

Shijin Yu[a], Jiahao Tong[a], Ying Wei[a,b], Tianrui Chen[a,b], Xuannan He[a,b], Huiqiang Sui[a], Cuiyun Li[b], Hua Zhu[a*], Qiuyun Fu[b*], LingBing Kong[c*]

[a] School of Mechanical and Electrical Engineering, Jingdezhen Ceramic University, Jingdezhen 333001, Jiangxi, China

[b] School of Optical and Electronic Information, Engineering Research Center for Functional Ceramics of the Ministry of Education, Huazhong University of Science and Technology, Wuhan, 430074, Hubei, China

[c] College of New Materials and New Energies, Shenzhen Technology University, Shenzhen 518118, Guangdong, China

*** Corresponding author**: zwchua@163.com (H. Zhu), fuqy@hust.edu.cn (Q. Fu), lbkongntunus@126.com (L. B. Kong)

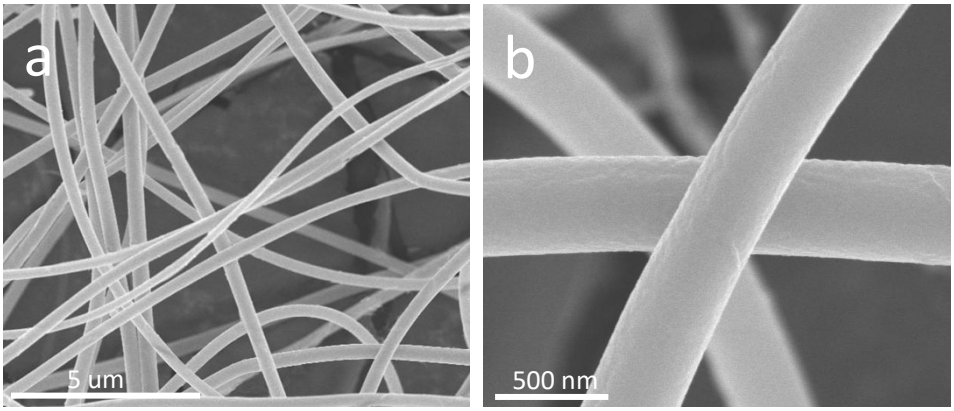

Fig.S1 SEM images of the as-spun Ni/Co compound nanofibers：(a) low magnification and (b) high magnification.

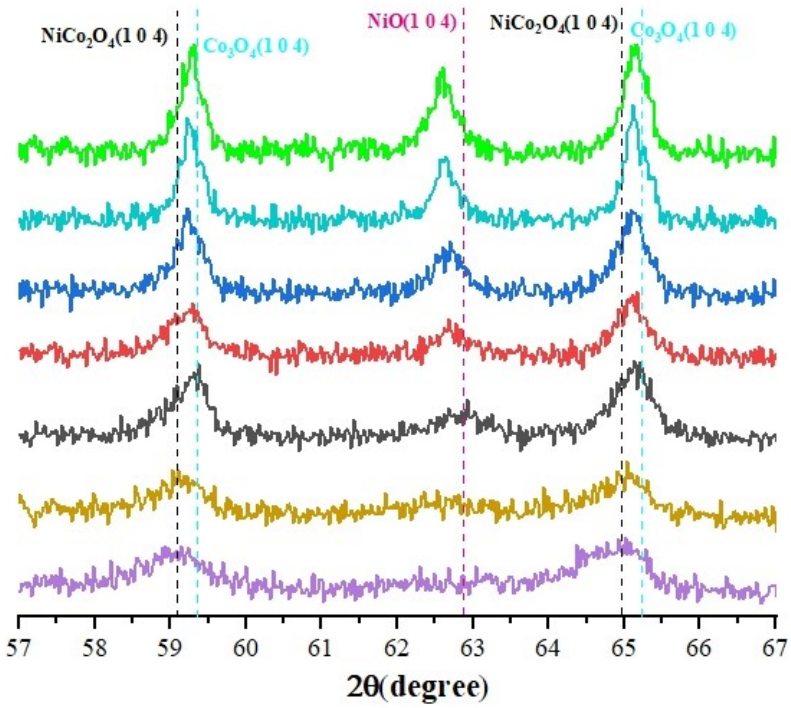

Fig.S2 Zoom-in XRD patterns (57°–67°) of the nanofiber annealed at different temperatures. The standard Bragg positions for NiO, Co_3O_4 and $NiCo_2O_4$ are marked.

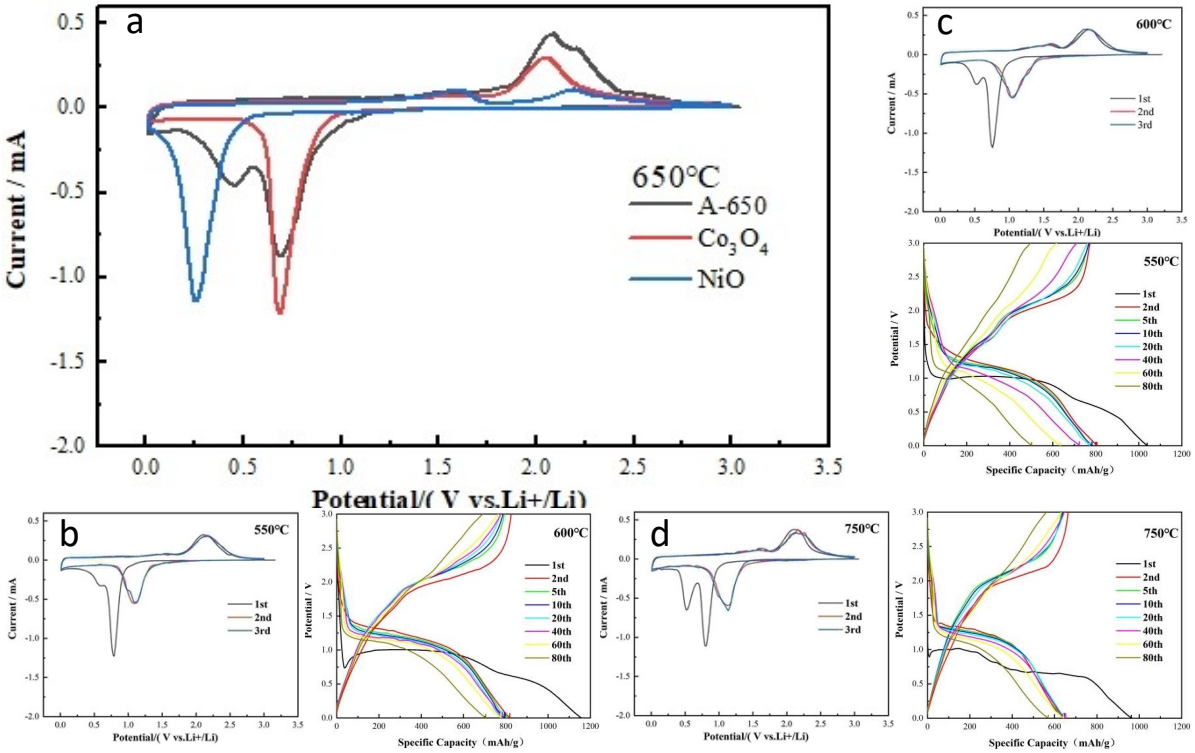

Fig.S3 (a) CV curves of A-650 sample, Co_3O_4 and NiO nanofiber electrodes. CV curves and charge-discharge curves of A-550 (b), A-600 (c) and A-750 (d) nanofiber electrodes.

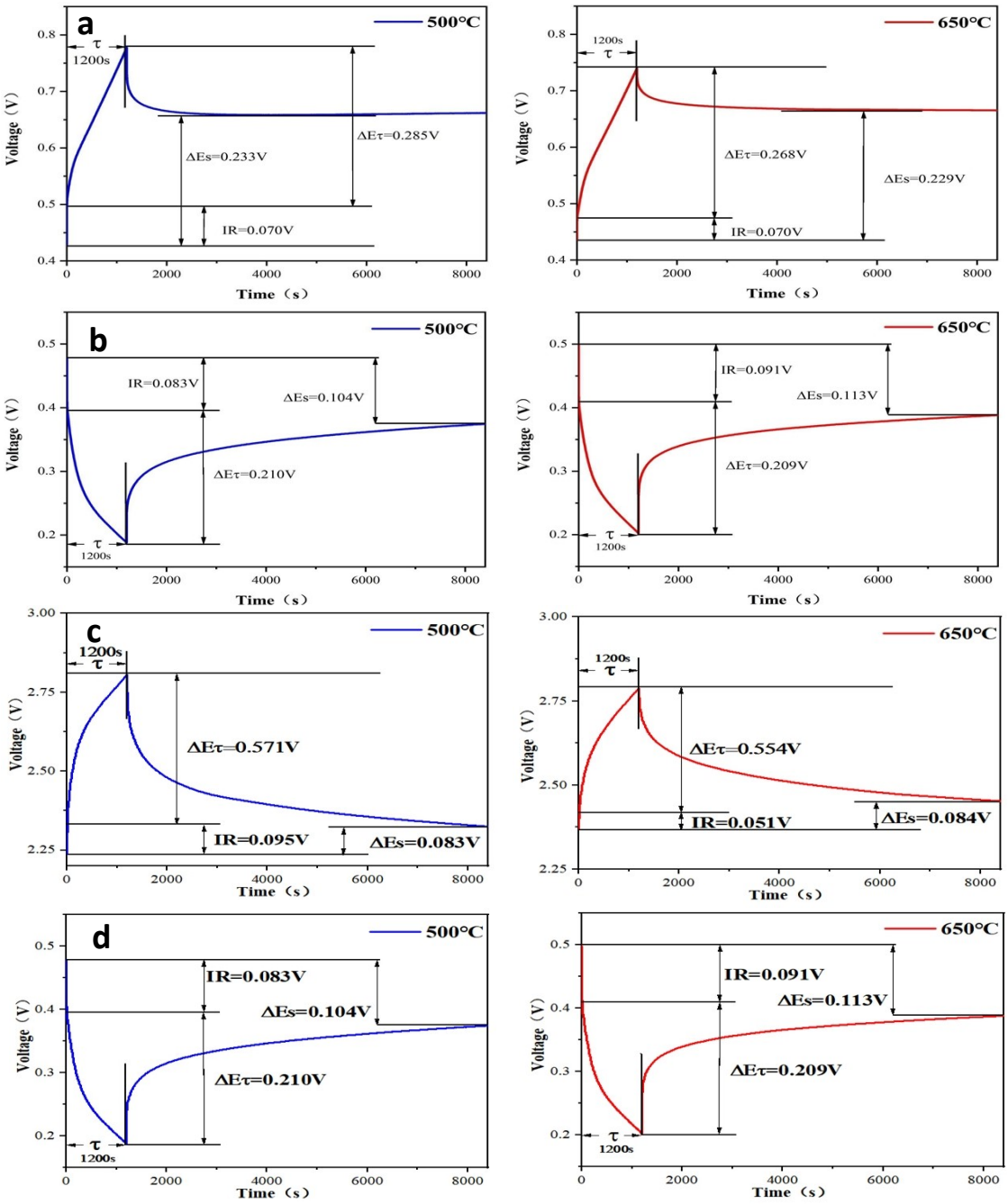

Fig. S4 polarized curves of A-500 and A-650 electrodes at different potentials during the charging-discharging process.

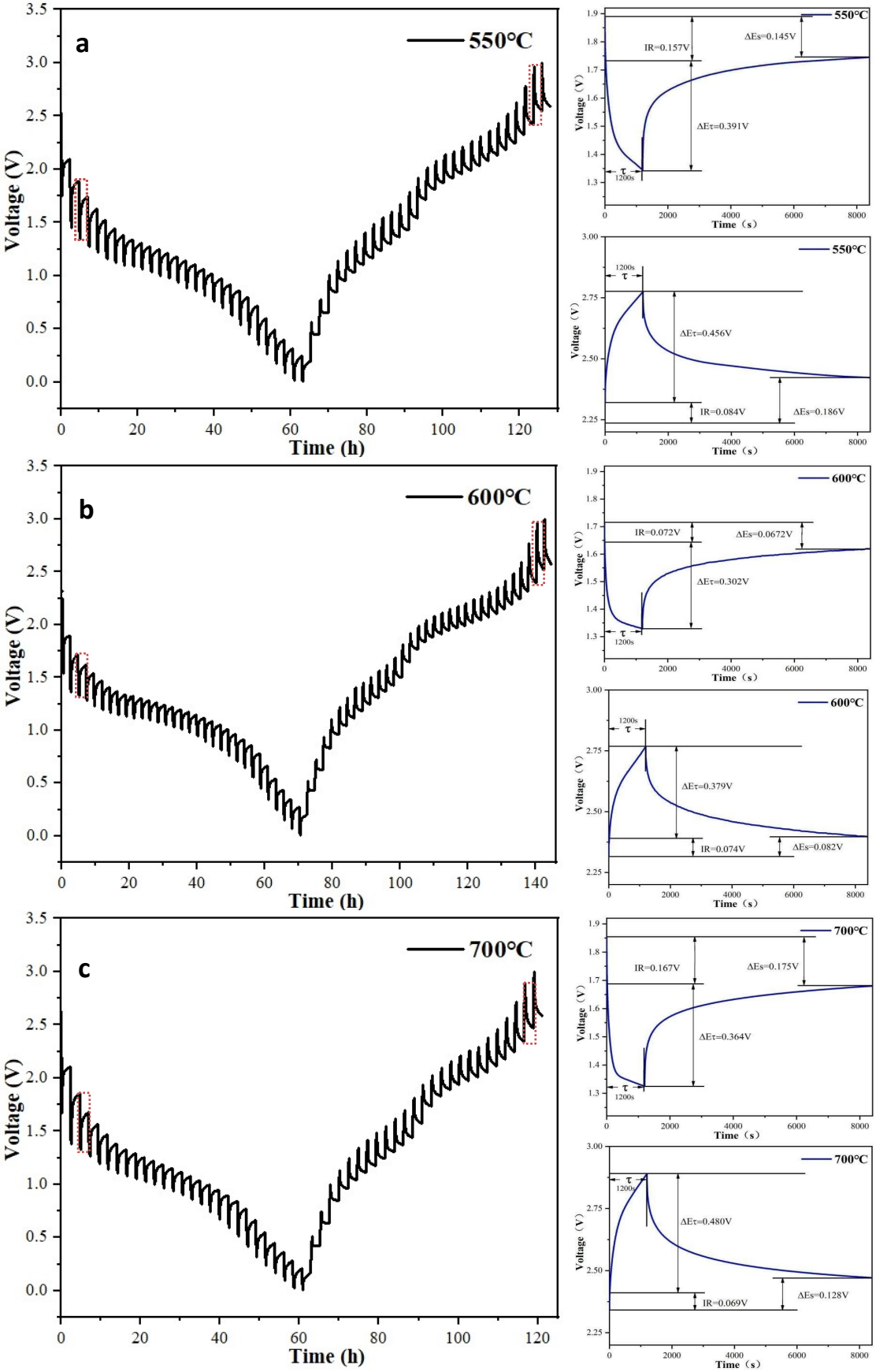
a
550°C
Voltage (V)
Time (h)
IR=0.157V
ΔEs=0.145V
ΔEτ=0.391V
τ
1200s
Time（s）
IR=0.084V
ΔEs=0.186V
ΔEτ=0.456V
b
600°C
IR=0.072V
ΔEs=0.0672V
ΔEτ=0.302V
IR=0.074V
ΔEs=0.082V
ΔEτ=0.379V
c
700°C
IR=0.167V
ΔEs=0.175V
ΔEτ=0.364V
IR=0.069V
ΔEs=0.128V
ΔEτ=0.480V

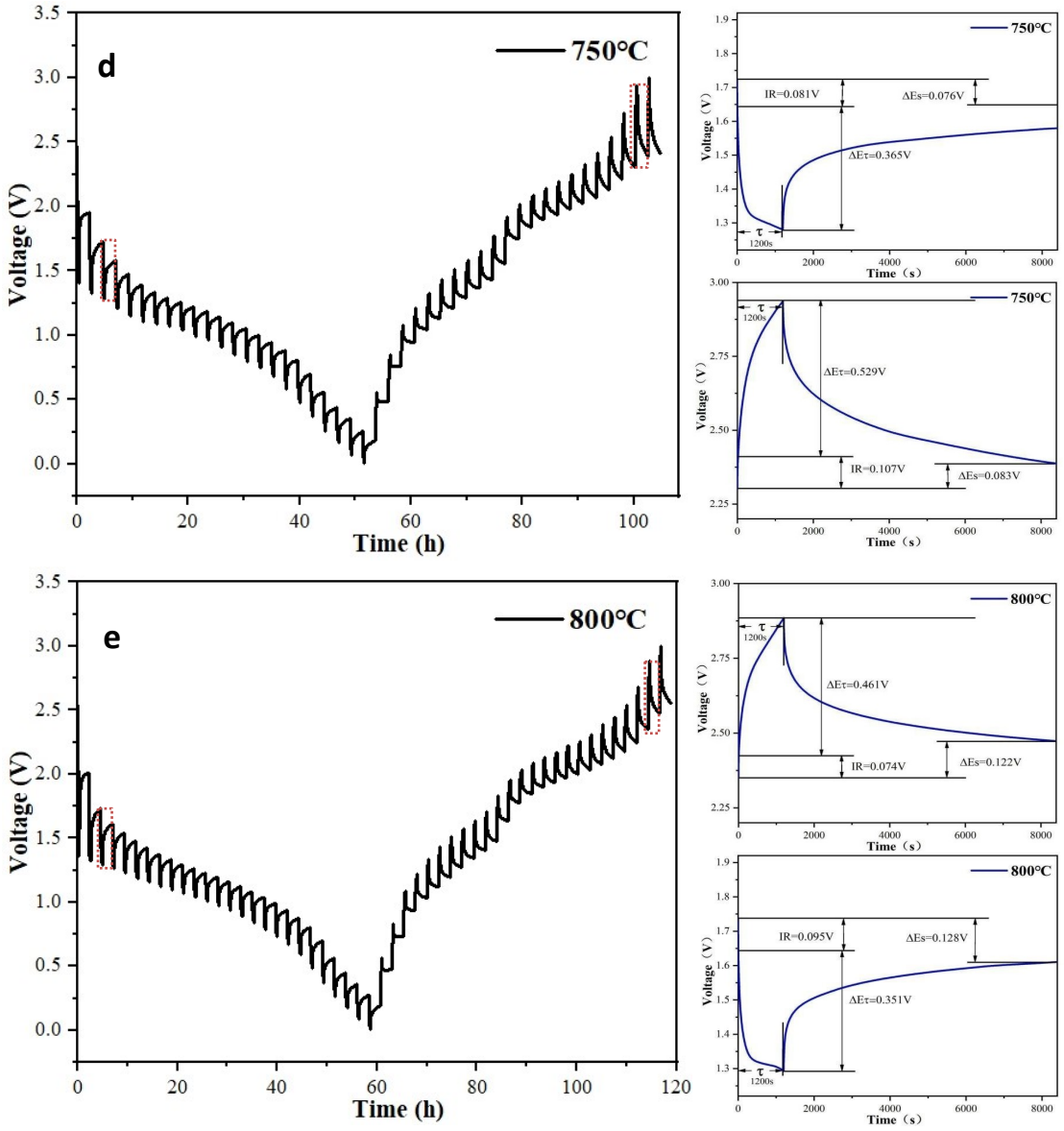

Fig. S5 GITT curves of the nanofiber electrodes: (a) A-550, (b) A-600, (c) A-700, (d) A-750 and (e) A-800.

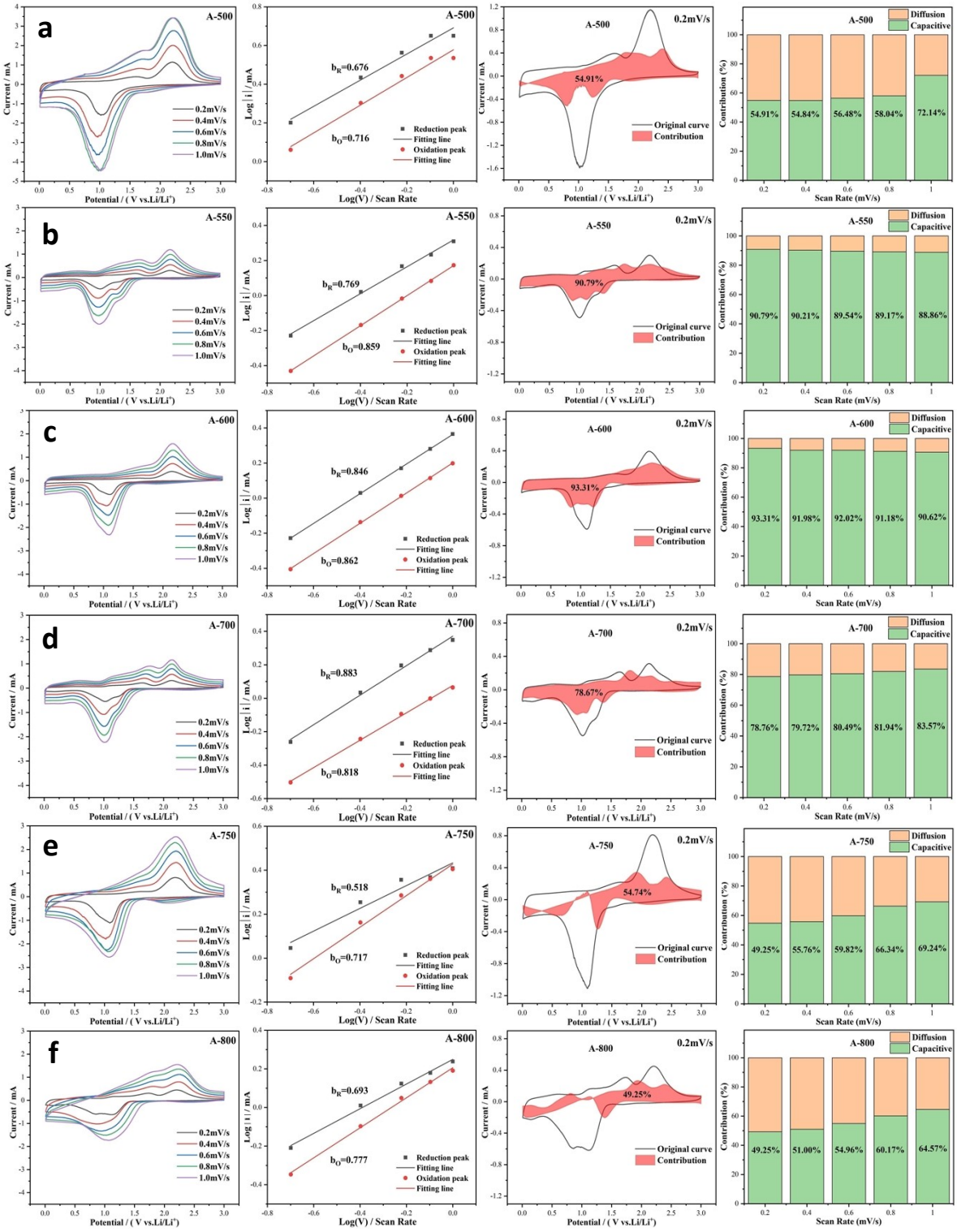

Fig.S6 CV curves and b values of the nanofiber electrodes at different scan rates, pseudocapacitive ratio at a scan rate of 0.2 mV s^{-1}， pseudocapacitive contribution at different rates: (a)A-500, (b) A-550, (c) A-600, (d) A-700, (e) A-750 and (f) A-800.

Table S1 Grain sizes of the nanofibers

Samples	A-500	A-550	A-600	A-650	A-700	A-750	A-800
Diameter (nm)	47.8	58.9	75.6	82.6	90.3	98.3	198.5

Table S2 Activation period and capacity boost of the electrodes

Samples	2th cycle capacity（mAh g^{-1}）	Maximum value of capacity（mAh g^{-1}）	Activation period (number of cycles)	Capacity boost （mAh g^{-1}）	Capacity boost rate (%)
A-500	881.6	1055	38	173.4	19.67%
A-550	805.5				
A-600	818.8				
A-650	890.1	1081.4	61	187.6	21.08%
A-700	882.7	1009.7	39	127	14.39%
A-750	639.1	663.9	26	24.8	3.88%
A-800	826.8	914.2	16	87.4	10.57%

Table S3 Capacity recovery of the electrodes after the current density is returned from 2000 mA g^{-1} to 100 mA g^{-1} and the capacity increase during the following 10 cycles

Samples	Cycling capacity at 2000 mA g^{-1} current density (mAh g^{-1})	Capacity returns to 100 mA g^{-1} (mAh g^{-1})	Recovered capacity value (mAh g^{-1})	Recovered capacity ratio (%)	10th cycle capacity returns to 100 mA g^{-1} (mAh g^{-1})	10 cycles of capacity boost after restoring 100mA g^{-1} (mAh g^{-1})	10 cycles of capacity boost ratio after restoring 100mA g^{-1} (%)
A-500	470.3	914.2	443.9	94.4	968.1	53.9	5.9
A-550	622.7	888.9	266.2	42.8	965.3	76.4	8.6
A-600	745.5	877.5	132.0	17.7	936.8	59.4	6.8
A-650	556.3	944.2	387.9	69.7	1067.9	123.7	13.1
A-700	573.6	887.3	313.7	54.7	977.2	89.9	10.1
A-750	526.3	831.4	305.0	58.0	912.4	81.0	9.7
A-800	322.8	711.0	388.2	120.3	737.0	26.0	3.7

Table S4. Performances of the $NiCo_2O_4$ based electrodes in this work and previous reports.

Sample	Specific capacity obtained from the cycling test	Ref.
Pristine $NiCo_2O_4$		
$NiCo_2O_4$ nanofiber with $NiO/Co_3O_4/NiCo_2O_4$ heterostructure	1081.4 mAh g^{-1} at 100 mA g^{-1} after 62 cycles	This work
$NiCo_2O_4$ flowers	939 mAh g^{-1} at 100 mA g^{-1} after 60 cycles	1
$NiCo_2O_4$ hollow spheres	706 mAh g^{-1} at 200 mA g^{-1} after 100 cycles	2
$NiCo_2O_4$ nanosheets	805 mAh g^{-1} at 200 mA g^{-1} after 60 cycles	3
$NiCo_2O_4$ nanocactus arrays	520 mAh g^{-1} at 120 mA g^{-1} after 100 cycles	4
$NiCo_2O_4$ submicron particle	384 mAh g^{-1} at 60 mA g^{-1} after 50 cycles	5
$NiCo_2O_4$ polyhedra	1050 mAh g^{-1} at 100 mA g^{-1} after 60 cycles	6
single-crystalline $NiCo_2O_4$ nanoribbons	1198 mAh g^{-1} at 200 mA g^{-1} after 60 cycles	7
$NiCo_2O_4$ composites		
RGO/$NiCo_2O_4$@carbon nanofibers	1712 mAh g^{-1} at 500 mA g^{-1} after 300 cycles	8
$NiCo_2O_4$@carbon fibers	639 mAh g^{-1} at 200 mA g^{-1} after 100 cycles	9
$NiCo_2O_4$@carbon nanofiber	778 mAh g^{-1} at 222.5 mA g^{-1} after 300 cycles	10
$NiCo_2O_4$@graphene	985 mAh g^{-1} at 200 mA g^{-1} after 60 cycles	3
$NiCo_2O_4$@Au nanotubes	732.5 mAh g^{-1} at 100 mA g^{-1} after 200 cycles	11
$NiCo_2O_4$@graphene	886 mAh g^{-1} at 500 mA g^{-1} after 450 cycles	12
NiO@graphene nanofibers	571 mAh g^{-1} at 100 mA g^{-1} after 50 cycles	13

Table S5 Comparative analysis of overpotential of A-500 and A-650 electrodes

	samples	ΔEτ(V)	ΔEs(V)	ΔEτ-ΔEs(V)
The second charging cycle	A-500	0.285	0.233	0.052
	A-650	0.268	0.229	0.039
The last second charging cycle	A-500	0.571	0.083	0.488
	A-650	0.554	0.084	0.470
The third discharging cycle	A-500	0.41	0.148	0.262
	A-650	0.376	0.158	0.218
The last forth discharging cycle	A-500	0.210	0.104	0.106
	A-650	0.209	0.113	0.096

Table S6 Resistance values of the electrodes

samples	A-500	A-550	A-600	A-650	A-700	A-750	A-800
$R_{ct}(\Omega)$	690.7	530.5	495.8	270.2	509.6	598.3	803.2
$Z_w(\Omega)$	180.2	79.4	110.4	15.6	124.9	43.3	75.1

References

1. L. Li, Y. Cheah, Y. Ko, P. Teh, G. Wee, C. Wong, S. Peng and M. Srinivasan, *Journal of Materials chemistry A*, 2013, **1**, 10935-10941.
2. L. Shen, L. Yu, X.-Y. Yu, X. Zhang and X. W. Lou, *Angewandte Chemie International Edition*, 2015, **54**, 1868-1872.
3. C. Zhang and J.-S. Yu, *Chemistry – A European Journal*, 2016, **22**, 4422-4430.
4. J. Cheng, Y. Lu, K. Qiu, H. Yan, J. Xu, L. Han, X. Liu, J. Luo, J.-K. Kim and Y. Luo, *Scientific Reports*, 2015, **5**, 12099.
5. D. Darbar, M. R. Anilkumar, V. Rajagopalan, I. Bhattacharya, H. I. Elim, T. Ramakrishnappa, F. I. Ezema, R. Jose and M. V. Reddy, *Ceramics International*, 2018, **44**, 4630-4639.
6. Y. Xia and H. Wang, *Ionics*, 2016, **22**, 159-166.
7. B. Li, J. Feng, Y. Qian and S. Xiong, *Journal of Materials Chemistry A*, 2015, **3**, 10336-10344.
8. R. Li, H. Ke, C. Shi, Z. Long, Z. Dai, H. Qiao and K. Wang, *Chemical Engineering Journal*, 2021, **415**, 128874.
9. M. L. Hsiao and C. T. Lo, *International Journal of Energy Research*, 2020, **44**, 8606-8621.
10. J. Zhang, R. Chu, Y. Chen, H. Jiang, Y. Zhang, N. M. Huang and H. Guo, *Nanotechnology*, 2018, **29**, 125401.
11. J. Zhu, Z. Xu and B. Lu, *Nano Energy*, 2014, **7**, 114-123.
12. S. Liu, J. Wu, J. Zhou, G. Fang and S. Liang, *Electrochimica Acta*, 2015, **176**, 1-9.
13. B. Yuan, J. Li, M. Xia, Y. Zhang, R. Lei, P. Zhao and X. Li, *Materials Research Express*, 2020, **7**, 115007.